Small Format Digital Imaging for Informal Settlement Mapping

Jonathan Li, Yu Li, Michael A. Chapman, and Heinz Rüther

Abstract

Recent advances in technology and wider commercial applications have promoted the remote sensing and airborne mapping communities to take a closer look at digital imaging and its advantages over conventional film-based, large-format aerial photography. In this paper, we focus on the potential of high-resolution, digital color imagery acquired from an airborne small-format digital camera for rapid mapping of complex urban informal settlements. We discuss the example of automated building extraction using a novel color edge extractor developed with similarity-based color morphology and report on investigations into the use of this low-cost digital imaging option for rapid spatial data acquisition of informal settlements under dynamic conditions. Results from our work suggest that the approach taking advantage of color information to generate attributed edges to hypothesize shack roof outlines by exploiting the fuzzy similarity measure and color morphology is a potential new avenue to automatically extract buildings from high-resolution color digital imagery.

Introduction

Informal settlements, also called squatter settlements or shantytowns, refer to generally unplanned, poorly structured, densely populated, and irregularly developed settlements, comprised of communities housed in self-constructed shelters under conditions of informal or traditional land tenure. Informal settlements are typically the product of an urgent need for shelter by the urban poor in developing countries and are characterized by a dense proliferation of small makeshift shelters, the utilization of diverse building materials (such as plastic, tin sheeting, and wood), the degradation of the local ecosystem (for example, erosion, poor water quality, and poor sanitation) and severe social problems. About 20 percent of the people in South Africa are living in informal settlements. There is a strong need for improvement and upgrading of informal settlement living conditions through the provision of infrastructures (e.g., water and electricity supplies, and basic road or sewerage systems) which in turn creates an urgent need for timely and accurate geospatial data. Typical tasks requiring geospatial data include monitoring settlement growth (both infill and expansion), relocating residents to formal housing, *in situ* upgrading settlements through the provision of infrastructure, and managing both natural disasters (e.g., flood and fires), and the local socioeconomic environment (Mason and Rüther, 1997). To this end, the need for cost-effective processes to acquire spatial data is especially relevant in the context of informal settlements in South Africa.

For technologies to be effective in an informal settlement environment, they must be low cost, both in data acquisition and information extraction, fast and reliable, simple to use, and as far as possible, based on off-the-shelf technologies. In contrast to these requirements, the acquisition of spatial data of informal settlements has been based on the black-and-white, film-based, large-format (230 mm $\times$ 230 mm) aerial photography. Film-based aerial cameras, by their very nature, are comprised of mechanical moving parts that require precise calibration and careful maintenance to ensure they remain within the necessary mapping accuracy standards. High-quality images can be produced by setting precise shutter speeds, adjusting the aperture, and selecting the lens filters. However, film is subject to deformation and tonal differences, which are difficult to correct (Artes, 2004). Film-based aerial photographs have to be converted by using an automated photogrammetric scanner (e.g., Vexcel UltraScan® 5000, Z/I Imaging PhotoScan®) into a digital form to allow further computer-assisted photogrammetric processing to generate digital map products. Moreover, film-based, large-format aerial photography is uneconomical for flying over the often relative small, densely populated areas covered by informal settlements and is too expensive to employ on a regular basis for tasks such as change detection and map revision. Alternative imaging sources and mapping techniques are therefore needed.

Although the use of 1 m resolution commercial satellite imagery (e.g., Ikonos) for local planning becomes viable, such imagery is not expected to fully suffice as a source for generating a layout plan at a scale of 1:2,000 or larger. For example, it remains to be seen whether water points and power lines can be reliably extracted from such satellite imagery. Under such circumstances, 1 m satellite imagery may be supplemented by higher resolution, small-format digital aerial imagery using a concept of multi-resolution coverage (Mason and Fraser, 1998).

Digital sensors offer more flexibility for image quality. An operator can view a digital image on-the-fly immediately after exposure and adjust the radiometry (balancing image illumination for brightness, darkness, and variation of brightness across the image) to fit changing atmospheric conditions. The time required to process digital imagery is significantly shorter than that needed to process standard film reducing the turnaround time from weeks or days to a matter of hours. Digital cameras can produce a sharper

J. Li, Y. Li, and M.A. Chapman are with the Department of Civil Engineering, Ryerson University, 350 Victoria Street, Toronto, Ontario, Canada M5B 2K3 (junli@ryerson.ca).

H. Rüther is with the Department of Geomatics, University of Cape Town, Private Bag, Rondebosch 7701, Cape Town, South Africa.

Photogrammetric Engineering & Remote Sensing
Vol. 71, No. 4, April 2005, pp. 435–442.

0099-1112/05/7104–0435/$3.00/0

image than scanned film, and the potential for image correlation allows for automatic measurements to be undertaken with acceptable accuracy. An all-digital approach to providing geospatial information is the way of the future. The use of a small-format digital camera as an aerial imaging system for commercial use has been fairly limited. Most examples in photogrammetric mapping applications are based on the Kodak DCS® and MegaPlus® series (e.g., Light, 1997; Mason *et al.* 1997; Maas, 1998; Chandler *et al.*, 2001). The relative low cost of the camera and the flexibility for platforms (light aircraft or helicopter) ensure that this imaging option is economic and practical for frequent map revision of informal settlements. The acquired digital data can in turn be photogrammetrically processed on a low cost PC-based system. The array size has been a restrictive factor for standard mapping applications, generally producing images in the region of up to 2,036 pixels × 3,060 pixels. But, it is found that such small-format imaging systems are attractive for small-area informal settlement mapping.

According to Mason and Fraser (1998)'s investigation, one of the predominant data requirements in local level informal settlement management is spatial inventory of structures (shacks). Shack data are required for many applications ranging from dwelling counts for residential density analysis to precise shack footprint measurement for in-situ upgrading. Given the size of many informal settlements (many are composed of thousands of shacks) and the need for frequent inventory updating in the face of rapid change due to settlement expansion, in fill or shack relocation and extension, there is a strong need for automated shack extraction tools. Ideally, these tools should be implemented on a PC and simple to use. In the following discussion, we examine the development towards automated shack extraction from high-resolution digital color imagery. In contrast to the previous development which focused on semi-automated methods (Baltsavias and Mason, 1997; Li, 2000; Rüther *et al.*, 2002), our study attempts the development of an automated solution to shack extraction by taking advantage of digital image processing techniques; although, the combination and integration of the models and strategies with human interaction to develop semi-automatic methods is of major practical importance. The objective of this paper is to present an effective color edge detection method for automatically extracting building roof outlines from high-resolution color digital imagery. The significance results of this study are: (a) the use of color information of the imagery; (b) providing a general method to design the edge detector based on color morphology, and (c) the proposed color edge extractor is image-independent, i.e., it can be used for different types of color imagery with different scenes acquired from either airborne mobile mapping systems or satellite imaging sensors.

In the following sections, we will first describe the study site and dataset used for our study, then present a novel color edge detection approach on the basis of exploiting fuzzy similarity measure and color morphology followed by illustrating and discussing the results of automated shack extraction.

Study Site and Data Set

Over the last decade, Cape Town, as well as many other big cities in South Africa, has experienced a dramatic increase of migrants from their economically neglected former homelands, mainly Transkei and Ciskei. This migration has resulted in the mushrooming of informal settlements on free urban land, in and around the city (Li, 2000). By the end of 1990s, there were estimated to be 120 informal settlements in the Cape Metropolitan Area (CMA). Two sites were chosen as the study areas for the UrbanModeler project carried out in the Department of Geomatics at the University of Cape Town, due to their difference in size, proximity to economic nodes, conflict potential within the settlement and with formal residents, outside support, age, and the application of the city's housing policy. This project was also guided by practical engagement in two informal settlement upgrading cases: (a) GIS support of the community representative body in Marconi Beam in facilitating that settlement's relocation to a low-cost housing site; and (b) information system support of the Weltevreden Valley low-cost housing development.

The first application of KODAK DCS460C digital camera for informal settlement mapping was carried out under the UrbanModeler project in the area of Marconi Beam in 1996. Figure 1 shows a mosaic of two DCS460C images covering the Marconi Beam informal settlement on 26 May 1996. At that time, its dimensions were approximately 465 m × 220 m covering an area of roughly 7.8 ha. A survey in December 1996 showed that approximately 5,700 people lived in 1,278 shacks in Marconi Beam (Li, 2000).

The KODAK DCS460C is a high-resolution (6 million pixels) digital camera working in a normal color mode. The camera has a specific CCD array (2,036 pixels × 3,060 pixels, 9 μm × 9 μm pixel size, corresponding to a frame size of 18.5 mm × 27.6 mm) mosaic structure that requires a dedicated processing algorithm for production of a three-band image. In the DCS460C the color chip (indicated by "C") records visible radiation in three bands. Kodak uses their patented filtration pattern of the individual CCD elements, providing alternate red, green, and blue in a special sequence. These images, stored on an internal PCMCIA hard-drive in DCS format are around 6 MB in size. The image in the DCS format is interpolated using a Kodak interpolation algorithm to produce a 36-bit color image (12 bits per color). During the process of converting the image from the DCS format to one of the standard image format, e.g., TIFF, the image is reduced to 24-bit color. This gives a nominal size of 18.6 MB.

Figure 1. The study site – Marconi beam informal settlement, Cape Town, South Africa.

The DCS460c was flown onboard a Piper Arrow 200 light aircraft (with a custom-built mount fitted to a porthole below the passenger seat) over the Marconi Beam informal settlement at 520 m flying height to yield a 0.18 m ground pixel size. An imaging scale of close to 1:18 500 was adopted (Mason *et al.*, 1997). This provided an image footprint of about 510 m × 340 m and a stereo model area of close to 300 m × 340 m. The camera was connected using a SCSI interface to a laptop with precise time information provided by an onboard GPS receiver. GPS was used for providing coarse positioning for the strip, but actual image acquisition had to rely on the operator's visual judgment due to the low flying height and the low precision (±100 m) of the navigation device. In Marconi Beam, a strip was flown with five passes during which two DCS460c images were acquired per pass using a 28 mm lens at infinity focus, at *f*5.6 with a hot mirror filter. The hot mirror filter reduces near-infrared light, resulting in less noise and more accurate images. From the ten acquired images, a set of six images providing full stereo coverage of the Marconi Beam settlement were chosen for triangulation providing overlaps ranging between 62 percent and 90 percent.

In terms of photogrammetric data, the image products most sought from the DCS460c images for informal settlement mapping are comprised of georeferenced, rectified, or orthorectified image maps (mosaiced where necessary). While it is acknowledged that these products display disadvantages against those from film-based, large-format aerial photographs (in terms of format size and resolution), the economics and ease of acquisition of small-format digital imagery are very compelling, especially for frequent data updating in the case of informal settlements under dynamic conditions. With small-format aerial imagery, however, one is often required to give careful consideration to geometric image correction. For example, the "rubber sheeting" rectification approach for aerial imagery is unlikely to yield satisfactory results for the DCS460c images until the frequent large lens distortion error is compensated. This problem impacts directly upon mosaicing. Of course, if rigorous photogrammetric procedures were adopted, such problems would not arise. The well-known instability of interior orientation with the DCS460c is not of too much consequence in rapid mapping of informal settlements The detailed evaluation of the DCS460c camera's potential of photogrammetric mapping can be found in Mason *et al.* (1997).

The results obtained, nevertheless support the proposition that small-format digital cameras can provide low-cost aerial imagery (a flight mission costing a few hundred US dollars), with sufficient cartographic quality to support informal settlement mapping at a scale of 1:2 000. With a ground resolution of 0.2 m most thematic details of interest could be extracted. A move to higher ground resolution is accompanied by practical problems that include a decrease in the already limited image footprint, and a compromise of flight geometry due to camera recycling times (approximately six seconds for the DCS460c).

Methodology

Mapping from remotely-sensed imagery often aims at the automatic detection and extraction of objects with the homogeneous surface cover of known type. By using nadir airborne digital imaging, visible shack roofs can be detected. It is reasonable to assume that the operation of shack detection is equivalent to the detection of roofs from aerial imagery. Such an assumption will not lose its generality because in many applications, such as map revision and GIS data updating, the existence of a shack is of importance. Therefore, automated shack detection problem can be simplified as a roof detection problem. The accuracy of such a process can be enhanced by edge detection. In this paper, we focus on the development of a color edge detection method for automating the detection and extraction of shacks as the predominant data requirement. In next section, we describe the definitions of fuzzy similarity measure and color morphology, which are the foundation of our color edge detection method.

Fuzzy Similarity Measure

To model the relationship among colors is a basic and important task in color image processing. The commonly used methodology is to treat the color at each pixel as a vector (Machuca and Phillips, 1983), and define an ordering of color vectors. Although a number of different schemes to order vector data have been proposed (Barnett, 1976), there is no generally accepted scheme, since there is no notion of the natural order in a vector space as in a one dimension case. In order to characterize the relationship among colors, instead of ordering color vectors, the similarity among colors is employed; the concept of color similarity is proposed, and the fuzzy-based color similarity measure is defined in our previous work (Li, 2004). According to human vision perception, the defined measure is based on the following assumption: similarity among colors is *short-range* and *fuzzy*. The so-called short-range similarity means that similar colors in the color space should be concentrated on a small neighborhood. The concept of fuzzy similarity can conclude that the similarity between two colors always shows much more uncertainty, and depends on individual sensation. As a result, the best way to describe the similarity among colors is to define a fuzzy-based measure, which characterizes the nature of short-range. In this paper, the similarity measure is given by

$$\mu(\boldsymbol{V}_i,\boldsymbol{V}_j) = e^{-k_1 d(\boldsymbol{V}_i,\boldsymbol{V}_j)} \cos\big(k_2 \theta(\boldsymbol{V}_i,\boldsymbol{V}_j)\big) \tag{1}$$

where k_1, $k_2 = [0, \infty)$, $d(\boldsymbol{V}_i, \boldsymbol{V}_j)$ is the Euclidean distance between the color vectors $\boldsymbol{V}_i = [V_{iR}, V_{iG}, V_{iB}]$ and $\boldsymbol{V}_j = [V_{jR}, V_{jG}, V_{jB}]$, and $\theta(\boldsymbol{V}_i, \boldsymbol{V}_j)$ is the angle induced by the correlation of the color vectors $\boldsymbol{V}_i$ and $\boldsymbol{V}_j$. Then we have

$$d(\boldsymbol{V}_i,\boldsymbol{V}_j) = \big((V_{iR} - V_{jR})^2 + (V_{iG} - V_{jG})^2 + (V_{iB} - V_{jB})^2\big)^{1/2} \tag{2}$$

$$\theta(\boldsymbol{V}_i,\boldsymbol{V}_j) = a\cos\frac{V_{iR}V_{jR} + V_{iG}V_{jG} + V_{iB}V_{jB}}{(V_{iR}^2 + V_{jG}^2 + V_{iB}^2)^{1/2}(V_{jR}^2 + V_{jG}^2 + V_{jB}^2)^{1/2}} \tag{3}$$

where V_{iR} (V_{jR}), V_{iG} (V_{jG}), V_{iB} (V_{jB}) are the red, green, and blue components of the color vector $\boldsymbol{V}_i$ ($\boldsymbol{V}_j$) in the RGB color space.

It is worthy to notice that the proposed color similarity measure proposes the following properties.

- *Ascending*: The similarity measure between two colors should have a larger value if they are more similar comparing with the one between other two colors.
- *Convex*: Given two colors, if there are other two colors that locate between them, then the similarity measure between the latter is larger than that between the former.
- *Identical*: The similarity measure should be equal to 1 when two colors are the same.
- *Symmetric*: Two colors should have the same similarity no matter their order.

Similarity-based Color Morphology

According to the color similarity described above, we define color morphology based on the assumption that the colors

representing an object in a color image are much more similar than those for other objects. In fact, it is true for most of scenes. Under the above assumption, our color morphological operations should be able to smooth the colors in the same object and at the same time "shrink" or "expand" the objects to detect their geometric structure.

Let $\boldsymbol{V} = \{\boldsymbol{V}_1, \boldsymbol{V}_2, \ldots, \boldsymbol{V}_n\}$ be a color vector set with n color vectors. The set of the most dissimilar color vector pair $\boldsymbol{V} \times \boldsymbol{V}_{DS}$ induced in $\boldsymbol{V}$ can be defined as

$$\boldsymbol{V} \times \boldsymbol{V}_{DS} = \{(\boldsymbol{V}_i, \boldsymbol{V}_j)\big|_{\mu(\boldsymbol{V}_i,\boldsymbol{V}_j) = \min\limits_{1\le k,l\le n} \mu(\boldsymbol{V}_k,\boldsymbol{V}_l)}\}. \tag{4}$$

From $\boldsymbol{V} \times \boldsymbol{V}_{DS}$, a color vector pair is randomly selected as the most dissimilar color vector pair $(\boldsymbol{V}_{DS1}, \boldsymbol{V}_{DS2}) \in \boldsymbol{V} \times \boldsymbol{V}_{DS}$. The *maximum* (*minimum*) color vector $\boldsymbol{V}_{max}$ ($\boldsymbol{V}_{min}$) in ($\boldsymbol{V}_{DS1}$, $\boldsymbol{V}_{DS2}$) is defined as

$$\boldsymbol{V}_{max} = \boldsymbol{V}_{DSi}\big|_{\|\boldsymbol{V}_{DSi}\| \ge \|\boldsymbol{V}_{DSj}\|\ i,j=1,2} \tag{5}$$

$$\boldsymbol{V}_{min} = \boldsymbol{V}_{DSi}\big|_{\|\boldsymbol{V}_{DSi}\| < \|\boldsymbol{V}_{DSj}\|\ i,j=1,2} \tag{6}$$

where $\|\cdot\|$ is a norm chosen as the measure of the magnitude of a vector.

All color vectors in $\boldsymbol{V}$ can be classified as two so-called "similar color classes" $\boldsymbol{CL}_1$ and $\boldsymbol{CL}_2$, which can be expressed as

$$\boldsymbol{CL}_1 = \{\boldsymbol{V}_i\big|_{\mu(\boldsymbol{V}_i,\boldsymbol{V}_{min}) \ge \mu(\boldsymbol{V}_i,\boldsymbol{V}_{max}),\forall \boldsymbol{V}_i \in \boldsymbol{V}}\} \tag{7}$$

$$\boldsymbol{CL}_2 = \{\boldsymbol{V}_i\big|_{\mu(\boldsymbol{V}_i,\boldsymbol{V}_{min}) < \mu(\boldsymbol{V}_i,\boldsymbol{V}_{max}),\forall \boldsymbol{V}_i \in \boldsymbol{V}}\}. \tag{8}$$

The most similar vectors $\boldsymbol{V}_{\boldsymbol{CL}_1}$ ($\boldsymbol{V}_{\boldsymbol{CL}_2}$) in $\boldsymbol{CL}_1$ ($\boldsymbol{CL}_2$) are determined by

$$\boldsymbol{V}_{\boldsymbol{CL}_1} = \boldsymbol{V}_i\Big|_{\boldsymbol{V}_i \in \boldsymbol{CL}_1 \text{ and } \sum_{j=1}^{|\boldsymbol{CL}_1|} \mu(\boldsymbol{V}_i,\boldsymbol{V}_j) = \max\limits_{1\le k\le |\boldsymbol{CL}_1|} \{\sum_{j=1}^{|\boldsymbol{CL}_1|} \mu(\boldsymbol{V}_k,\boldsymbol{V}_j)\}} \tag{9}$$

$$\boldsymbol{V}_{\boldsymbol{CL}_2} = \boldsymbol{V}_i\Big|_{\boldsymbol{V}_i \in \boldsymbol{CL}_2 \text{ and } \sum_{j=1}^{|\boldsymbol{CL}_2|} \mu(\boldsymbol{V}_i,\boldsymbol{V}_j) = \max\limits_{1\le k\le |\boldsymbol{CL}_2|} \{\sum_{j=1}^{|\boldsymbol{CL}_2|} \mu(\boldsymbol{V}_k,\boldsymbol{V}_j)\}} \tag{10}$$

where $|\boldsymbol{CL}_1|$ and $|\boldsymbol{CL}_2|$ are the numbers of colors in $\boldsymbol{CL}_1$ and $\boldsymbol{CL}_2$, respectively.

The above procedure to obtain the most similar vectors is defined as the infimum operator $\wedge$ and the supremum operator $\vee$.

$$\wedge \boldsymbol{V} = \wedge \{\boldsymbol{V}_1, \boldsymbol{V}_2, \cdots, \boldsymbol{V}_n\} = \boldsymbol{V}_{\boldsymbol{CL}_1} \tag{11}$$

$$\vee \boldsymbol{V} = \vee \{\boldsymbol{V}_1, \boldsymbol{V}_2, \cdots, \boldsymbol{V}_n\} = \boldsymbol{V}_{\boldsymbol{CL}_2} \tag{12}$$

From the definition given in Equation 11, it is obvious that the operator $\wedge$ outputs the so-called "most centrally located" vector $\boldsymbol{V}_{\boldsymbol{CL}_1}$ in $\boldsymbol{CL}_1$, which has the maximum sum of the defined fuzzy similarity measure between it and all the other vectors in $\boldsymbol{CL}_1$. And the $\vee$ operator results in most centrally located vector $\boldsymbol{V}_{\boldsymbol{CL}_2}$ in $\boldsymbol{CL}_2$, which has the minimal sum of the defined fuzzy similarity measure between it and all the other vectors in $\boldsymbol{CL}_2$. Based on the infimum and supremum operators, the color morphological operators can be described as follows.

Let $\boldsymbol{V}_C = \{\boldsymbol{V}_{C1}, \boldsymbol{V}_{C2}, \ldots, \boldsymbol{V}_{CN}\}$ be a color vector set formed by all N color vectors of a color image C, the $\boldsymbol{V}_P$ is a subset of $\boldsymbol{V}_C$ from a window centered at the pixel with index p. The color dilation δ_C, color erosion ε_C, color closing χ_C, and color opening o_C of the color image C are, respectively, given by

$$\delta_C(\boldsymbol{V}_C) = \{\vee \boldsymbol{V}_P, p = 1,2,\ldots,N\} \tag{13}$$

$$\varepsilon_C(\boldsymbol{V}_C) = \{\wedge \boldsymbol{V}_P, p = 1,2,\ldots,N\} \tag{14}$$

$$\chi_C(\boldsymbol{V}_C) = \varepsilon_C(\delta_C(\boldsymbol{V}_C)) \tag{15}$$

$$o_C(\boldsymbol{V}_C) = \delta_C(\varepsilon_C(\boldsymbol{V}_C)). \tag{16}$$

From the above definition, the color dilation (erosion) of the color image C keeps the three steps. First, the window centered at a selected pixel p is constructed which consists of the neighborhood pixels around p. Second, the infimum and supremum operations are performed to the color vector set $\boldsymbol{V}_P$ corresponding to the window centered at each pixel p in the color image processed. Third, the original color vector is replaced with the resultant color vector from the second step for each pixel.

Color Edge Detection Approach

Edge detectors are widely used on grayscale imagery as the first step in image segmentation. In this section we present a color edge detection method based on the proposed color morphological operations. Edge detection is based upon the detection of local variations which mainly correspond to the boundaries of homogeneous objects in the image. An edge, also known as a discontinuity, in a signal is usually defined as a transition in the intensity or amplitude of that signal. Most of the existing edge detection approaches aim at finding a measure of strength and direction of gradient in the image characteristics, and then, by applying a fixed or dynamic threshold, to define edges (Zhu *et al.*, 1999).

Our color edge detection method is based on measuring the similarity or dissimilarity between two color images by following three consequent stages. In the first stage, a pair of dual morphological operations is chosen which extend or reduce the contours of objects in color imagery efficiently. In the second stage, the similarity between the resultant images for two chosen operations is calculated by using the similarity measure between two color images. And, the result of the measure is represented as a grayscale edge image, which indicates the potential edges. In the last stage, the edges are extracted by thresholding the grayscale edge image resulted from the second stage. Finally, a binary edge image is obtained. The process flow of our color edge detection method is shown in Figure 2.

Definition of Color Edge

The discontinuity of the brightness is normally used to define edges in grayscale imagery. However, the situation in the case of color imagery is different. Several definitions of color edges have been proposed (Pratt, 1991). For example, one of such definitions ignores discontinuities in hue and saturation that occur in regions of constant luminance with which a color edge may exist, if and only if, the luminance field contains an edge. The second way to define a color edge is to check if an edge exists in any of its constituent primary components. The third definition is based on forming the sum of gradients of the primary values or some linear or nonlinear color component. A color edge may exist if the gradient exceeds a threshold.

Unlike the definitions of color edges given in Pratt (1991), we use fuzzy color edges to develop our color edge extraction method. We consider each pixel as a potential color edge point having a membership to indicate the degree to which the pixel belongs to an edge.

Definition of Similarity Measure Between Two Color Images

According to the similarity measure between two color vectors, the similarity measure between two color images can be described as follows.

Let $\mu(\boldsymbol{V}_i, \boldsymbol{V}_j)$ be the similarity measure between the color vectors $\boldsymbol{V}_i$ and $\boldsymbol{V}_j$ in the RGB color space, and $C1$ and $C2$ are two color images with N pixels and all colors form the color vector sets $\boldsymbol{V}_{C1} = \{\boldsymbol{V}_{C11}, \boldsymbol{V}_{C12}, \ldots, \boldsymbol{V}_{C1N}\}$ and $\boldsymbol{V}_{C1} = \{\boldsymbol{V}_{C21},$

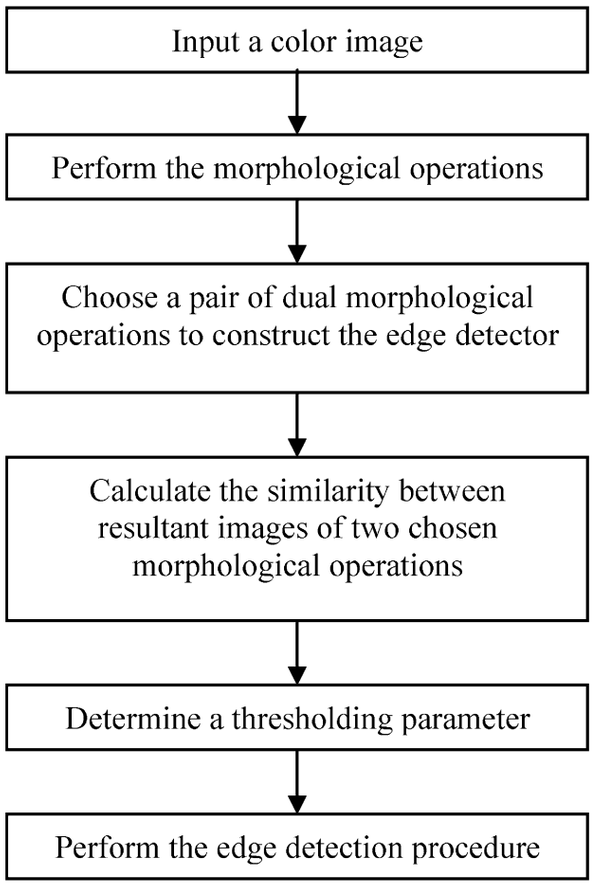

Figure 2. Process flow of our color edge detection method.

$\boldsymbol{V}_{C22}, \ldots, \boldsymbol{V}_{C2N}\}$, respectively. The similarity measure between $C1$ and $C2$ is defined as a scalar set $\boldsymbol{M}$, that is,

$$\boldsymbol{M} = \{M_1, M_2, \ldots, M_N\} = \{\mu(\boldsymbol{V}_{C11}, \boldsymbol{V}_{C21}), \mu(\boldsymbol{V}_{C12}, \boldsymbol{V}_{C22}), \ldots, \mu(\boldsymbol{V}_{C1N}, \boldsymbol{V}_{C2N})\} \quad (17)$$

where $M_i = \mu(\boldsymbol{V}_{C1i}, \boldsymbol{V}_{C2i})$ is the similarity measure between the color vectors $\boldsymbol{V}_{C1i}$ and $\boldsymbol{V}_{C2i}$.

Definition of the Edge Detector

Based on the similarity measure between two color images defined above, and let a be a selected threshold, $0 \leq a < b \leq 1$, the fuzzy similarity based edge detector (*FSED*) can be defined as a scalar set

$$FSED = \{FSED_i = \begin{cases} 1, & M_i \leq a \\ 0, & otherwise \end{cases}\} \quad (18)$$

where $FSED_i = 1$ defines color edges, $M_i = \mu(\boldsymbol{V}_{C1i}, \boldsymbol{V}_{C2i})$ is the similarity measure between the color vectors $\boldsymbol{V}_{C1i}$ and $\boldsymbol{V}_{C2i}$ from two color images resulted from two dual morphological operations.

Results and Discussion

Three experiments were carried out with the Marconi Beam dataset and the results are presented successively in this section. Three subsections of the 1: 18500 scale DCS460c color digital imagery were used to test our color edge detection method. Each color image tested has a size of 150 pixels × 150 pixels and 24 bits per pixel (see Figure 3). A 5 × 5 window size was applied for color morphological operations.

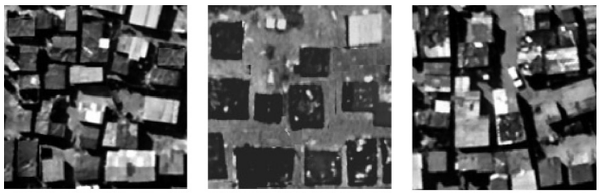

(a) (b) (c)

Figure 3. Three test images: (a) 0.5 threshold for edge similarity, (b) 0.3 threshold for edge similarity, (c) 0.1 threshold for edge similarity.

Edge Detection and Shack Extraction

In the experiments, the parameters k_1 and k_2 for all morphological operators were taken as 0.001 and 0.2, and k_1 and k_2 for similarity measures between images were set as 0.01 and 0.2, respectively, to design the fuzzy similarity edge detector (*FSED*).

In order to design the *FSED*, a pair of dual morphological operations should be selected first. In this study, the dilation-original images pair was chosen to construct the *FSED*. The similarity measure between the selected image pair was calculated with Equation 17, and the results are represented by a grayscale image as shown in Figure 4, in which each gray level corresponds to a similarity measure and indicates the degree to which the level belongs to an edge.

In order to extract shack roof outlines, the threshold that controls the pixels belonging to the edges should be determined. By observation, the thresholding parameters (see Table 1) were chosen to construct the *FSED*. The binary images of the edges extracted by the *FSED* are shown in Figure 5.

Figure 4. Grayscale images representing the fuzzy similarity measures between the original images (Figure 3) and the dilated images.

TABLE 1. OPERATION PAIR AND THRESHOLDING PARAMETERS

Color Images	Morphological Operation Pair	Thresholds for Edge Similarity
Figure 3a	Dilation-Original	0.5
Figure 3b	Dilation-Original	0.3
Figure 3c	Dilation-Original	0.1

Figure 5. Binary images of the extracted edges of shack roofs with noise.

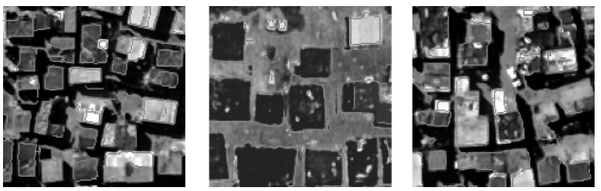

Figure 8. Extracted shack roof outlines overlaid on the input images.

It can be observed from Figure 5 that the extracted edges of shack roofs are contaminated by noise caused by other objects that have similar colors or due to less color uniformity of some shack roofs. In order to reduce the noise, a series of binary directly morphological operations were used (Li *et al.*, 2002). Figure 6 shows the shack edges obtained after filtering the binary edge images depicted in Figure 5 using the binary morphological operators and the selected thresholding parameters listed in Table 1. Visual comparison of Figures 5 and 6, the results of filtering binary images shown in Figure 5 with the angle interval of 3° and structuring elements 2×1, 5×1, and 4×1 applied to Figures 5a, b, and c, respectively, demonstrate that the directed binary dilation is effective to remove the noise.

The shack roof outlines were further delineated applying the thinning algorithm (Zhang and Suen, 1984) to the filtered edge images shown in Figure 6 and the results of thinning are shown in Figure 7.

For the purpose of verification, the extracted shack roofs (outlined in black) are overlaid on the corresponding original images. The results of overlaying are shown in Figure 8. A visual evaluation gives the impression that the detected shack roofs match the shapes of the building roofs in the images quite well.

As shown in Figure 8, some edges belonging to non-shack objects have also been extracted. There is a need for manual editing to remove those non-shack edges. Although the extracted shack roof outlines obviously not fully satisfactory, our method represents a significant saving in labor and a step towards automation. The results of this study clearly point to the need for multi-cue integration algorithms as reliable results cannot be achieved using a single image cue (e.g., color was used in this study) alone. In a multi-cue algorithm, each extraction technique provides information which can be added or assimilated into an overall interpretation of the scene.

The same procedures have been applied for processing the color image to extract formal buildings with a regularly shaped roof and a homogenous color (see Figure 9a). Comparison to Figure 8, a better performance of our method has been demonstrated when it is applied to extract formal buildings with a homogenous color (see Figure 9f).

Our method has not been able to accurately delineate building roofs in the same way a human operator could do. However, as illustrated in Figures 8 and 9, final building roof outlines are close enough to true shack roof edges implicitly, suggesting a post-editing step for applications requiring higher accuracies.

Figure 6. Shack hypotheses obtained after filtering.

Figure 7. Shack roof outlines delineated after thinning.

Conclusions and Outlook

A novel method of automated building extraction from color imagery obtained by the airborne small-format digital camera has been presented. Low-cost, high spatial resolution KODAK DCS460c digital camera onboard a light aircraft demonstrates the promise of a small-format digital imaging option for rapid mapping of informal settlements in the urban environment. We have shown that settlement objects (mainly shacks) can be automatically extracted from the DCS460c color imagery acquired by the DCS460c digital camera or its derivative color orthophoto imagery. An approach taking advantages of color information to generate attributed edges to hypothesize shack roof outlines has been described and tested. The framework presented, extends the concepts of mathematical morphology from existing binary and grayscale to color morphology, based on the proposed fuzzy similarity measure. The foundational and secondary operations of color erosion, color dilation, color opening, and color closing have also been defined. The new approach to color edge detection is vector preserving. We have illustrated the results of the application of the defined operations to color image edge detection by defining a fuzzy similarity edge detector based on the fuzzy similarity between a pair of morphological images. The proposed approach to building extraction in the complex urban informal settlement scenes was considered acceptable with a significant reduction of the need for human support. The fact that all building roof outlines together with some non-building edges in the study areas have been extracted, may be attributed the scene and shack complexity, i.e., to the unstructured nature of informal settlements scenes. Under

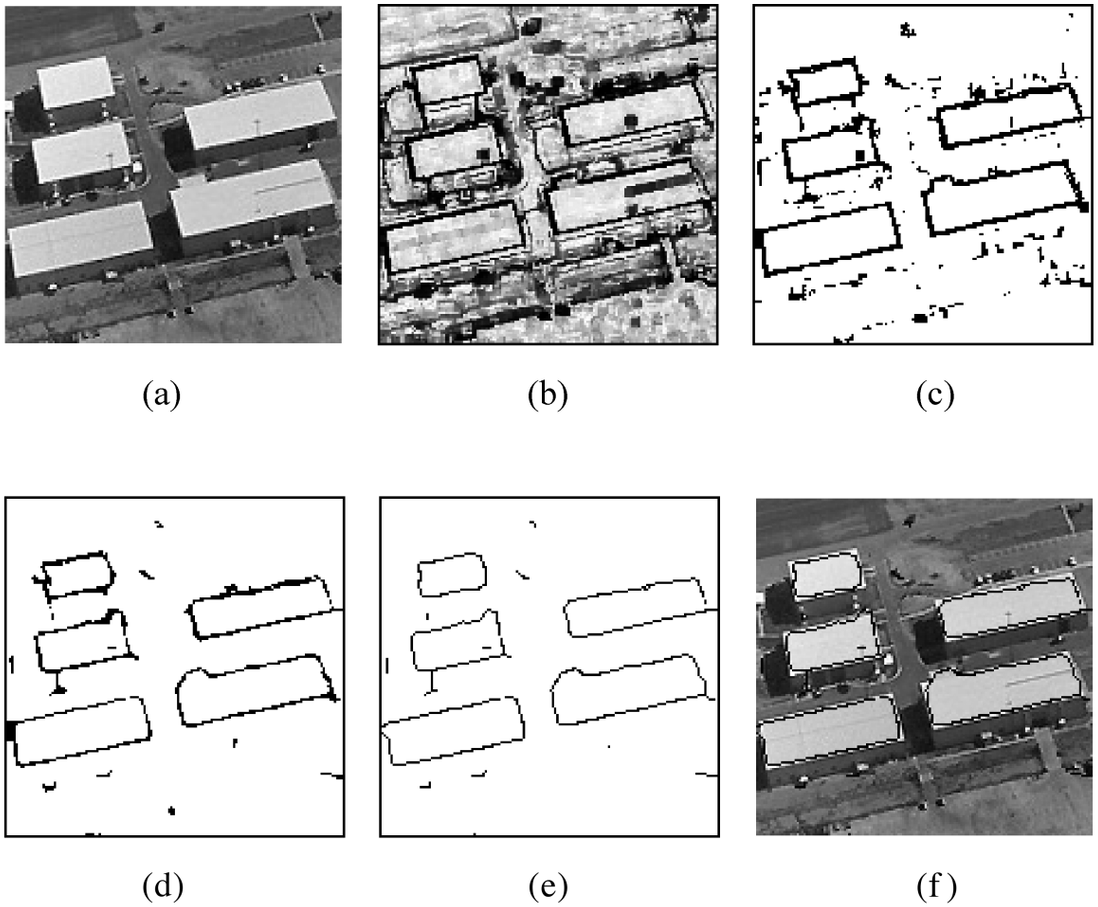

Figure 9. Process and results of the automated extraction of regularly shaped buildings: (a) input image, (b) detected edges, (c) edges after thresholding, (d) roof outlines after filtering (e) roof outlines after thinning, (f) extracted roof outlines overlaid on the input image.

the more structured scene conditions with formal buildings, the method performed better. The development of a generic building extraction method that can perform well under diverse scene conditions has been difficult to achieve to date, and remains a considerable challenge.

Acknowledgments

The research on the development of color edge detector was partially supported by a Natural Sciences and Engineering Research Council of Canada (NSERC) discovery grant. The acquisition of the KODAK DCS460C digital images of informal settlements was funded by the Foundation for Research Development of South Africa. The authors would also like to thank the anonymous reviewers for their valuable comments.

References

Artes, F., 2004. Medium-format digital cameras come of age, *Earth Observation Magazine*, 13(6):16–19.

Baltsavias, E.P., and S.O. Mason, 1997. Automated shack reconstruction using integration of cues in object space, *International Archives of Photogrammetry and Remote Sensing*, 32(3–4W2): 96–105.

Barnett, V., 1976. The ordering of multivariate data, *Journal of Royal Statistical Society A*, 3:318–355.

Chandler, J.H., K. Shiono, P. Rameshwaren, and S.N. Lane, 2001. Measuring flume surface for hydraulics research using a Kodak DCS460, *The Photogrammetric Record*, 17 (97):39–61.

Li, J., 2000. *Informal Settlement Modeling Using Digital Small-Format Aerial Imagery*, Ph.D. Dissertation, University of Cape Town.

Li, J., Y. Li, and H. Dong, 2002. Automated extraction of urban road networks from IKONOS imagery using a fuzzy mathematical morphology approach, *International Archives of Photogrammetry, Remote Sensing and Spatial Information Sciences*, 34(2II):259–263.

Li, Y., 2004. *Fuzzy Similarity Measure and Its Applications to High-Resolution Colour Remote Sensing Image Processing*, M.A.Sc. Thesis, Ryerson University, Toronto.

Light, D.L., 1997. A digital 3k × 2k array camera for reconnaissance and mapping, *Proceedings of the Annual Convention of ASPRS and ACSM*: 21p.

Maas, H.-G., 1998. On the accuracy potential of large format solid state matrix sensor cameras onboard an aircraft, *International Archives of Photogrammetry and Remote Sensing*, 32(I):20–25.

Machuca, R., and K. Phillips, 1983. Application of vector fields to image processing. *IEEE Transactions on Pattern Analysis and Machine Intelligence*, 5:316–329.

Mason, S.O., and C.S. Fraser, 1998. Image sources for informal settlement management, *The Photogrammetric Record*, 16(92):331–345.

Mason, S., and H. Rüther, 1997. Managing informal settlements spatially, *South African Journal of Geo-information*, 17(3):67–72.

Mason, S., H. Rüther, and J. Smit, 1997. Investigation of the Kodak DCS460 digital camera for small-area mapping, *ISPRS Journal of Photogrammetry and Remote Sensing*, 52(5):202–214.

Pratt, W.K., 1991. *Digital Image Processing*, 2nd Edition, John Wiley & Sons, New York.

Rüther, H.H., M. Martine, and E.G. Mtalo, 2002. Application of snakes and dynamic programming optimization technique in modeling of buildings in informal settlement areas, *ISPRS Journal of Photogrammetry and Remote Sensing*, 56(2002): 269–282.

Zhang, T.Y., and C.Y. Suen, 1984. A fats parallel algorithm for thinning digital patterns, *Communications of the ACM*, 27(3): 236–239.

Zhu, S., K.N. Plataniotis, and A.N. Venetsanopoulos, 1999. Comprehensive analysis of edge detection in color image processing, *Optical Engineering*, 38(4):612–625.